Non-thermal emissions from outer magnetospheric accelerator of pulsars

J.Takata* and H.-K. Chang†,**

*Institute of Astronomy and Astrophysics, and Theoretical Institute for Advanced Research in Astrophysics, Academia Sinica; and National Tsing Hua University, Taipei Taiwan
†Department of Physics, National Tsing Hua University, Hsinchu, Taiwan
** Institute of Astronomy, National Tsing Hua University, Hsinchu, Taiwan

Abstract. We study non-thermal emission process in pulsar magnetospheric accelerator (outer gap). We discuss emission process in optical through γ-ray bands. We solve the dynamics in the outer gap in the magnetic meridional plane, which includes the rotation and magnetic axes. We calculate the spectrum of the curvature and synchrotron processes. Using a three-dimensional geometrical model, we compute pulse profile and polarization characteristics. We compare the model results with the observations of the Vela pulsar and the Crab pulsar. We demonstrate that the observed multi-peak structure of the pulse profile observed by RXTE can be reproduced by the present study with the outward and inward emissions from the outer gap accelerator. The calculated polarization characteristics are in general consistent with the Crab optical data.

Keywords: pulsars, non-thermal emissions, theory
PACS: 97.60.Gb

INTRODUCTION

7 young pulsars have been known as the galactic sources of non-thermal emissions in optical through γ-ray bands (Thompson 2004). In the pulsar magnetospheres, charged particles are accelerated by the electric field parallel to magnetic field lines. The accelerating electric field arises in the region where the local charge density deviates from the Goldreich-Julian value. The high-energy particles emit the non-thermal photons via the curvature radiation, synchrotron radiation and inverse-Compton process. These non-thermal processes have been discussed with the polar cap model, the slot gap model and the outer gap model in the literature. The polar cap and slot gap models assume a strong acceleration regions near the stellar surface, while the outer gap model assumes an acceleration in outer magnetosphere. Because all three models can predict the properties of the γ-ray radiations measured by EGRET, the origin of the non-thermal emissions remains inconclusive.

Recent observations have also revealed properties of emissions in optical through X-ray bands. For example, multi-peak structure in pulse profiles of X-ray, UV and optical emissions of the Vela pulsar has been revealed (Romani et al. 2005), although the pulse profile in γ-ray bands has double peak structure. For the Crab pulsar, the polarization properties of the pulsed optical emissions were measured (Kanbach et al. 2005). INTEGRAL measured the highly-polarized soft γ-ray emissions from the Crab in off-pulse phase (Dean et al., 2008). These multi-wave length observations allow us to perform a comprehensive theoretical discussion for the physics of the non-thermal process in the pulsar magnetospheres.

The outer gap accelerator is one of the plausible site for the non-thermal processes. The predicted geometry of the outer gap accelerator naturally produces the double peak pulse profile in the γ-ray bands, while the polar cap model have to invoke both a small inclination angle and a small viewing angle measured from the rotational axis to reproduce the observed separation of the two pulse peaks. Recently, the pulsed emissions above 25 GeV from the Crab pulsar were measured by MAGIC telescope (The MAGIC collaboration: Aliu et al. 2008). The observed fluxes in EGRET through MAGIC bands are extrapolated with an exponential shape rather than a super-exponential shape. This indicates that emission happens far out in the magnetosphere.

In this paper, we study the non-thermal emissions in optical through γ-ray bands of the outer gap accelerator. We solve the dynamics in the outer gap in the magnetic meridional plane, which includes the rotation and magnetic axes. We calculate the spectrum of the curvature and synchrotron radiations. Using a three-dimensional geometrical model, we compute the pulse profile and polarization characteristics. We compare the model results with the observations of the Vela and Crab pulsars.

THEORETICAL MODEL

We consider a magnetized rotator in which an inclination angle α between the rotational axis and magnetic axis

CP1085, *High Energy Gamma-Ray Astronomy, 4th International Meeting on High Energy Gamma-Ray Astronomy*, edited by F. A. Aharonian, W. Hofmann, and F. M. Rieger

is smaller than 90°. In the outer gap, the positrons and electrons are accelerated outwardly and inwardly by the accelerating electric field.

Two-dimensional electrodynamic model

The stationary electric potential, Φ_{nco}, for the accelerating field in the observer frame is obtained from

$$\triangle\Phi_{nco}(\mathbf{r}) = -4\pi[\rho(\mathbf{r}) - \rho_{GJ}(\mathbf{r})], \quad (1)$$

where $\rho(\mathbf{r})$ is the space charge density, and $\rho_{GJ}(\mathbf{r})$ is the Goldreich-Julian charge density.

For the steady state, the continuity equations of the particles are written as

$$\mathbf{B}\cdot\nabla\left(\frac{v_{||}N_{\pm}(\mathbf{r})}{B}\right) = \pm S(\mathbf{r}), \quad (2)$$

where $v_{||} \sim c$ is the velocity along the field line, $S(\mathbf{r})$ is the source term due to the pair-creation process, and N_+ and N_- denote the number density of the positrons and electrons, respectively. In the outer magnetosphere, $\gamma + X \rightarrow e^+ + e^-$ pair-creation process contributes to the source term $S(\mathbf{r})$. We simulate the pair-creation process with a Monte Carlo method (Takata et al. 2006).

To solve the Poisson equation (1), we impose the boundary conditions on the four boundaries, which are called as inner, outer, upper and lower boundaries. The inner and outer boundaries are defined by the surfaces on which the accelerating electric field is vanishes, that is, $E_{||} = 0$. On the inner, upper and lower boundaries, the accelerating potential is equal to zero, that is, $\Phi_{nco} = 0$. On the inner boundary, because both conditions $E_{||} = 0$ and $\Phi_{nco} = 0$ are imposed, we can not know the position of the inner boundary in advance. We solve the position of the inner boundary with the dynamics. The lower boundary is defined by the last-open field line. The model parameters are locations of the upper and outer boundaries. The components of the current injections at the inner and outer boundaries are also model parameters.

Particle motion

To calculate the synchrotron and curvature radiation processes, we solve an evolution of the particle's momentum using the electric field distribution in the outer gap obtained by the method described in above section. The equation of motion for momenta of the parallel ($P_{||}/m_e c = \sqrt{\Gamma^2 - 1}\cos\theta_p$) and perpendicular ($P_{\perp}/m_e c = \sqrt{\Gamma^2 - 1}\sin\theta_p$) to the magnetic field lines are, respectively, described as

$$\frac{dP_{||}}{dt} = eE_{||} - P_{sc}\cos\theta_p, \quad (3)$$

and

$$\frac{dP_{\perp}}{dt} = -P_{sc}\sin\theta_p + \frac{c}{2B}\frac{dB}{ds}P_{\perp}, \quad (4)$$

where θ_p is the pitch angle, P_{sc} represents the radiation drag of the synchrotron and curvature radiation, and the second term on the right hand side on equation (4) represents the adiabatic change along the field line.

Three-dimensional geometrical model

The observed pulse profile and the polarization characteristics provide us an important tool for diagnose the geometry of the emission region in the magnetospheres. In particular, number of the peaks in a single rotational period and morphology of the pulse profiles at different energy bands will discriminate the emission models.

In the framework of the outer gap model, the peaks appear in the pulse profiles because the photons emitted various point pileup due to the effect of the special relativity correction; the aberration of the emitting direction and the flight time. To compute the pulse profile, we anticipate that the emission direction coincides with the particle motion. In the observer frame, the particle motion along the field lines in the north hemisphere is described by $\mathbf{v} = \pm v_0\mathbf{b} + v_{co}\mathbf{e}_{\phi}$, where the plus (or minus) sign represents the positrons (or electrons), v_0 is the velocity along the magnetic field line and is determined by the condition that $|\mathbf{v}| = c$, $\mathbf{b}$ is the unit vector of the magnetic field, for which we adopt a rotating dipole field in the observer frame, v_{co} is the co-rotating velocity, and $\mathbf{e}_{\phi}$ is the unit vector of the azimuthal direction. The emission direction, $\mathbf{n} \equiv \mathbf{v}/c$, is interpreted in terms of the viewing angle $\xi = n_z$ and the pulse phase $\Phi = -\phi_e - \mathbf{n}\cdot\mathbf{r_e}/R_{lc}$, where ϕ_e and r_e is the azimuthal emission direction and the radial distance to the emission point, respectively. We use a rotating magnetic dipole field in the observer frame to compute the pulse profile.

We calculate the polarization characteristics of the pulsed optical photons from the Crab pulsar using the three dimensional model developed by Takata et al (2007a,b). With the outer gap model, the pulsed optical photons are radiated via the synchrotron radiation of the secondary and tertiary pairs produced by the pair-creation process outside the gap. We assume that the radiation at each point are linearly polarized with degree of $\Pi_{syn} = (p+1)/(p+7/3)$, where p is the power law index of the particle distribution, and circular polarization is zero. For the power low index, we assume $p = 2$ (Takata et al. 2007a). The direction of the electric vector of the electro-magnetic wave toward the observer is parallel to the projected direction of the acceleration of the particle on the sky, that is, $\vec{E}_{em} \propto \vec{a} - (\vec{n}\cdot\vec{a})\vec{n}$, where $\vec{a}$ is the vector of the acceleration direction of the gyration motion.

RESULTS

Spectrum and pulse profile

In Figure 1, we compared the predicted spectrum for the Vela pulsar with the observed phase-averaged spectrum in optical through γ-ray bands. The model spectrum was calculated from the two-dimensional electrodynamic model. In Figure 1, the solid and dashed lines represent the spectra of the outwardly and inwardly emitted photons, respectively. The dotted line shows the spectrum of the total emissions. For each line, components of the curvature and the synchrotron radiations are combined. Although we did not demonstrate in Figure 1, the curvature (or synchrotron) radiation dominates above (or below) 10 MeV. From Figure 1, we see that the total spectrum (the dotted line) is consistent with the observations in whole energy bands.

We find that above 10 MeV, the outward curvature radiation by the out-going positrons is main radiation process for the Vela pulsar. This is because most of the pairs are created near the inner boundary. The created electrons and positrons are accelerated inwardly and outwardly by the electric field, respectively. The positrons created near the inner boundary are accelerated by almost whole potential drop in the gap, while the created electrons are accelerated by the potential drop only between the inner boundary and the point where they was created. As a result, the total radiation power is larger for the outward emissions than the inward emissions.

Below 10 MeV, we find that the synchrotron radiation of the in-going electrons also contributes to total emissions. In particular, the inward emissions are more important around 1 MeV bands. In X-ray bands, both the inward and outward emissions contribute to the total emissions. These results indicate that the morphology of the pulse profiles depends on the energy bands.

Figure 2 shows pulse profiles of the outward (solid line) and inward (dashed line) emissions calculated from the three-dimensional model. For the outward emissions, the pulse profile has two-peaks in a single period. The first and second peaks are, respectively, results for the pileup of the radiated photons at leading and trading parts of the gap according to the rotational direction. As dashed-line in Figure 2, the pulse profile of the inward emissions has also double peak structure. For the inward emissions, the first peak is created by the emissions from the trailing part of the gap, while the second peak is made by the emissions of the leading part of the gap.

From Figure 1, we see only outward emissions contribute to the total spectrum above 10 MeV. Therefore, the expected pulse profile has two-peaks in a single period, as the solid line in Figure 2 indicates. This predicted double peak structure is consistent with the EGRET

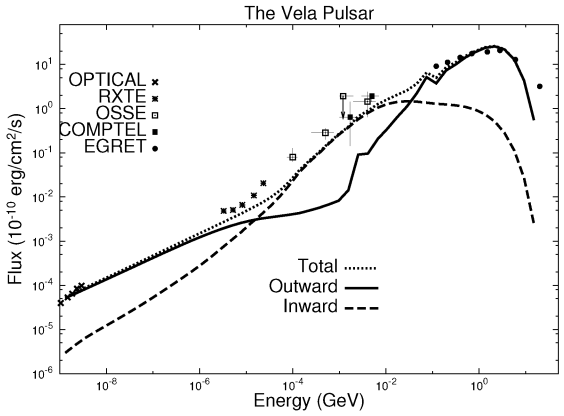

FIGURE 1. The spectrum of the synchrotron and curvature radiations of the Vela pulsar. The solid and dashed lines represent the spectra for the outwardly and inwardly emitted photons, respectively. The dashed line represents the total emissions. The results are for the inclination angle $\alpha = 60^\circ$.

observations. Although the previous geometrical studies have ignored the inward emissions to just avoid the multi-peak structure in γ-ray bands, we demonstrated with the electrodynamic study (Figure 1) that the inward emissions is weak in γ-ray bands.

In 1-10 keV bands, the calculated spectrum (Figure 1) shows that both inward and the outward emissions contribute to the total spectrum. In Figure 2, therefore, we expect the pulse profile is composed of the inward emission (solid line) and outward emissions (dashed line). The pulse profile has four peak in a single period. The predicted multi peak structure in X-ray bands is consistent with the observed pulse profile by RXTE for the Vela pulsar (Harding et al. 2002).

In 1-10 MeV bands, we also predicts multi peak structure as well as 1-10 keV bands, because both outward and inward emissions contribute to the total spectrum as Figure 1 shows. AGILE and/or Fermi telescopes will measure detail structure of the pulse profiles in about 10 MeV bands. In 10 keV-1 MeV bands, because the inward emissions dominate in the total emissions (Figure 1), we expect the double peak structure of the pulse profile. The pulse peaks in 10 keV-1 MeV bands will not be in phase with that of γ-ray bands, in which the outward emissions dominate in the total emissions.

Polarization

We applied the three-dimensional model to the Crab pulsar and calculated the polarization characteristics in optical bands. For the Crab pulsar, the emission process in the optical bands is synchrotron radiation of the sec-

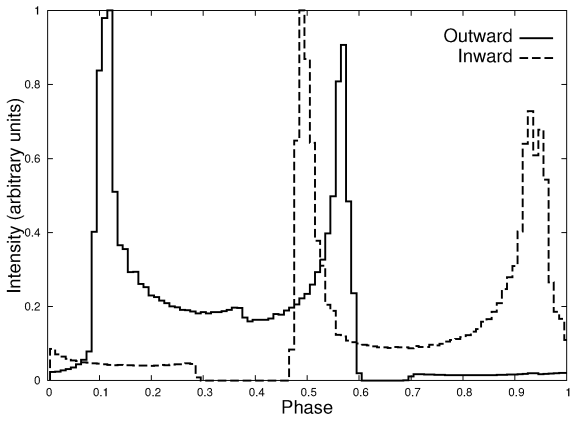

FIGURE 2. The pulse profiles of the Vela pulsar. The solid and dashed lines represent the expected pulse profiles of outwardly and inwardly emitted photons, respectively.

ondary and tertiary particles produced outside the gap. Figure 3 shows the calculated polarization characteristics at 1 eV. Top, middle and bottom panels show the pulse profile, the position angle of the polarization and the degree of the linear polarization. For the position of the inner boundary, we use the results of the two-dimensional electrodynamics study (Takata et al. 2007b), in which the outer gap starts from the radial distance of 65% of the distance to null charge surface. Figure 3 shows the results for the inclination angle of $\alpha = 50^\circ$, and the viewing angle $\xi \sim 100^\circ$. The viewing angle is chosen so that the predicted phase separation between the two peaks is consistent with the observed value $\delta\Phi \sim 0.4$ phase.

As seen in the calculated degree of the linear polarization, the synchrotron emissions of the on-pulse phase ($\Phi = 0 - 0.4$ in Figure 3) appear with a lower polarization degree than intrinsically assumed value ($\sim 70\%$) with the power low index $p = 2$. This depolarization is caused by the effects of the gyration motion. In the synchrotron case, the direction of the acceleration vector, and therefore the direction of the polarization depends on the phase of the gyration motion around the magnetic field. The overlap of the radiations from the particles with the different gyration phases causes the depolarization. For the pulsed emissions, the radiations from the particles with the different gyration phase may be observed at the same pulse phase, because of (i) the special relativistic corrections and (ii) the rotation of the magnetosphere. As a result, the emerging radiation from the pairs polarizes with a very low polarization degree ($\sim 10\%$) compared with the inartistic value. In off-pulse phase, the depolarization is weaker and the emerging radiation highly polarizes, because the radiations from the some range of gyration phases are not observed because the line of sight passes through the edge of the emission

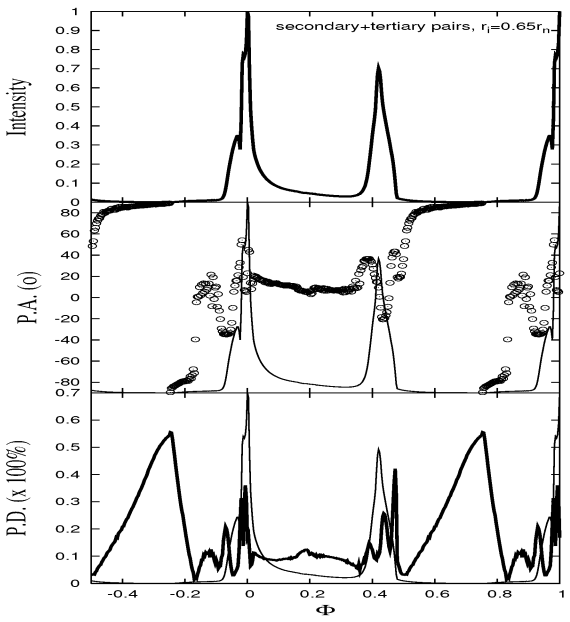

FIGURE 3. Predicted polarization characteristics for the pulsed optical photons from the outer gap accelerator of the Crab pulsar. The to, middle and bottom panels show the light curve, position angle of the polarization and the degree of the linear polarization. The results are for the inclination angle $\alpha = 50^\circ$ and the viewing angle $\xi = 100^\circ$.

regions.

In the polarization angle swing in the present model, the large swings appear at the both peaks, and the difference of the position angle between the off-pulse and the bridge phases is about 90 degree. These calculated polarization characteristics are in generally consistent with the Crab optical data for the emissions after subtraction of the DC level, which has the constant intensity at the level of 1.24% of the main pulse intensity.

REFERENCES

1. Dean A.J. et al., 2008., Sci, 321, 1183
2. Harding A.K., Strickman M.S., Gwinn C, Dodson R., Moffet D. & McCulloch P., 2002, ApJ, 576, 376
3. Kanbach G., Słowikoska A., Kellner S. & Steinle H., 2005. AIP Conf. Proc. Vol. 801, p. 306
4. Romani R.W., Kargaltsev, O. & Pavlov, G.G., 2005, ApJ, 627, 383
5. Takata J., Shibata S., Hirotani K. & Chang H.-K. 2006, MNRAS, 366, 1310
6. Takata J. & Chang H.-K., 2007a, ApJ, 670, 677
7. Takata J., Chang H.-K. & Cheng K.S., 2007 ApJ, 656, 1044
8. The MAGIC Collaboration: Aliu E. et al., 2008., astro-ph/0809.2998
9. Thompson D.J., 2004, in Cheng K.S., Romero G.E., eds, Cosmic Gamma Ray Sources. Dordrecht, Kluwer, p. 149